

## Chapter 2

### Selectivity

#### 2.1 Introduction

In Chapter 1, we began the discussion of selectivity. In brief review, when an ideal selective layer is exposed to a mixture of molecules, it interacts with those for which the layer is selective and rejects the other, interfering molecules. The selective layer itself can be homogeneous or can contain specific binding sites embedded in a matrix. An outline of the thermodynamics governing the equilibrium binding was given in Section 1.1.

#### 2.2 Equilibrium-Based Selectivity

The discussion up until now has been formulated in terms of the change of free energy. We have yet to consider the types of chemical interactions that may be involved. The interactions that are relevant are all weak interactions. They are summarized in Table 2.1, and arranged in order of decreasing strength. The covalent bond is shown only for comparison; otherwise, it has no function in the selectivity scheme.

The energies in Table 2.1 are listed as enthalpies ( $\Delta H$ ), but the driving forces in the chemical species/sensor interactions are really the changes of free energy ( $\Delta G$ ), which include the change of entropy ( $\Delta S$ ). At constant temperature, the two are related by (2.1).

$$\Delta G = \Delta H - T\Delta S \quad (2.1)$$

The higher the entropy change, the more negative the free energy change is and the more stable the system. Entropy is a measure of the randomness of the system (Appendix A).

There are two aspects of Table 2.1 that we need to pay attention to, in addition to the interaction energies. First is the effect of the dielectric constant. Because the

**Table 2.1** Approximate interaction energies.  $D$  is dielectric constant;  $\alpha$  is polarizability;  $\mu$  is dipole moment;  $r$  is distance;  $z$  is charge;  $\Theta$  is angle and  $I$  ionization energy (adapted from van Holde, 1985)

Type of Interaction	Distance relationship (nm)	Order of magnitude (kJ/mol)
Covalent bond	0.08–0.2	50–200
Hydrogen bond	0.1–0.3	20–150
Donor–acceptor	0.1–0.3	50–150
Ion–ion	$E \approx \frac{z_1 z_2}{Dr}$	90
Ion–dipole	$E \approx \frac{z_1 \mu_2 \cos \Theta}{Dr^2}$	15
Dipole–dipole (stationary)	$E \approx \frac{\mu_1 \mu_2}{Dr^3}$	$\pm 2$
Dipole–induced dipole	$E \approx \frac{z_1 \alpha_2}{Dr^4}$	2
Dispersion	$E \approx \frac{\alpha_1 \alpha_2}{r^6} \frac{I_1 I_2}{I_1 + I_2}$	2–4
CH <sub>3</sub> –CH <sub>3</sub>	<0.1	(1.2) <sup>a</sup>
Φ – Φ	<0.1	(5) <sup>a</sup>

<sup>a</sup>Means per mole unit coupling

nature of all these interactions is electrostatic, increasing the dielectric constant ( $D$ ) makes most of the interactions weaker. Second is the dependence of the interaction on distance, that is, the term ( $r$ ). The higher the power of  $r$ , the faster the interaction energy decays with distance between the molecule and its binding site. This is why weak interactions are also called *short-range interactions*. There is no distance dependence for donor–acceptor complexes, hydrogen bonds, or hydrophobic bonds, in which the bond length is fixed and typically on the order of tenths of nanometers. The significance of the short-range distance dependence is in the shape recognition, which is the most important reason for the high selectivity inherent in the so-called “lock-and-key” biological interactions. There, as we show, the geometry of the interaction plays a dominant role.

### 2.2.1 Shape Recognition

Living organisms are the ultimate sensing machines. In order to survive, an organism must accomplish three missions: to metabolize, to reproduce, and to process information. The latter means both information acquisition and processing. There are millions of chemical species in the environment, so the *selectivity* is of primary importance; the acquisition of “false signals” and/or their wrong interpretation could be anything from humorous to disastrous. The biological strategy to avoid such problems is to involve shape recognition, in other words, stereospecificity.

So, let us look at the geometry of the binding site and of the analyte in Fig. 2.1. We are interested in examining their geometrical fit, meaning: “shape recognition.” Within the system shown in Fig. 2.1, they are clearly in a more random configuration if they are not associated, because they have more degrees of freedom and therefore

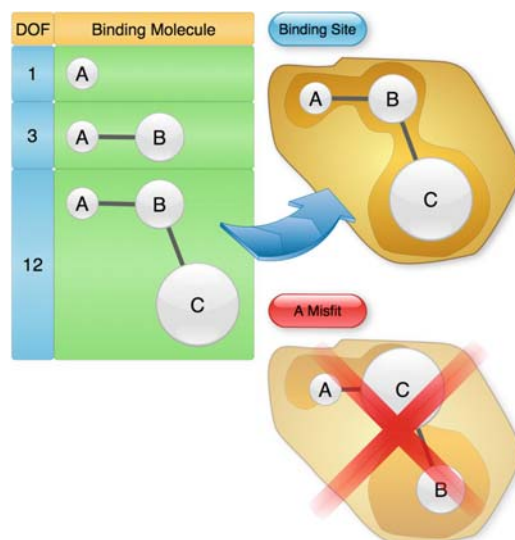


**Fig. 2.1** Shape recognition by the binding site increases with the geometrical complexity of the site. The number DOF represents the degrees of freedom that must be satisfied for a perfect fit to occur

higher entropy. In other words, on the entropy consideration alone they would be more stable if they were disassociated.

The only way they would be used in an active sensor is if the enthalpy decrease due to their association were high enough to compensate for the value of the term  $T\Delta S$  in (2.1). In this case, the “shape recognition” strategy will work only if there are negative-enthalpy-producing binding sites (exothermic) present inside the binding site *S*. Nature has, indeed, used this strategy in using hydrogen bonds, ionic bonds, charge-transfer complexes, and so on, inside the binding sites of hormone receptors and antibodies, among others. However, as can be seen from Table 2.1, most of the interactions fall off rapidly with the distance between the interacting entities (with the exception of the Coulombic ion–ion bond), and with the increase of the dielectric constant. The enthalpic interactions are common to many classes of compounds and as such would not be an optimum strategy for achieving high selectivity. So, is there a way out?

Let us consider the most regular object, a sphere. It has only one parameter that affects its potential to be selectively recognized: its size. There is only one “arrangement” that corresponds to a selective fit of the sphere to the binding site. Increasing the number of spheres in the arrangement can be conceptualized as increasing the number of atoms in the target molecule, which must correspond to an equal number and arrangement of spaces in the binding site if a selective fit is to be possible. Thus, if we now take two spheres connected with a solid rod (like a “dumbbell”) the number of possible “fits” (indicated in Fig. 2.1 by the term *A*) increases to three: two for the sizes of the balls and one for their distance. We take one more step in this progression and interconnect three balls of different size with

two links of different length. For this “molecule” the number of requirements for a perfect fit increases to 12: three for the diameters of the balls, two for the lengths of the links, one for the angle, and then double that for the configuration 1-2-3 or 1-3-2.

It is important to realize that only one configuration will fit the binding site. Therefore, it is generally true that, as the geometrical complexity increases, the number of possible misfits decreases and therefore the selectivity increases. Moreover, the “size of the ball” can be also interpreted as their ability to interact. Thus, even if the molecule fits the binding site geometrically, it must also match the type of enthalpic interaction belonging to that part of the binding site. For example, if Region 2 on the molecule is hydrophobic then it must be matched by the hydrophobic region in the binding site. Any other interaction will result in  $\Delta G > 0$ , which means repulsion. Therefore, a molecule approaching the binding site can be either attracted ( $\Delta G < 0$ ) or repulsed ( $\Delta G > 0$ ). So, in effect, a “mismatch” may actually have a negative contribution to the binding, and thus further enhance the overall recognition.

As we see from (2.1), the increase of entropy favors binding. This is the essence of the probably most important bond in biological systems, the hydrophobic bond. Figure 2.2a depicts the situation as it exists in vacuum, which is obviously not

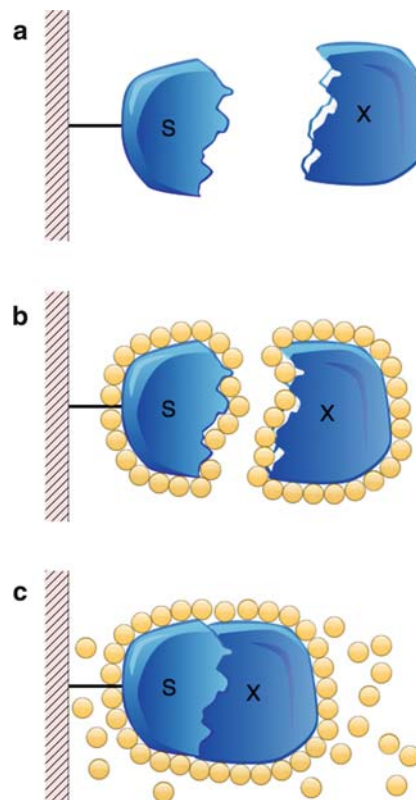


**Fig. 2.2** Entropic nature of the “hydrophobic” bond

a “typical” biological situation. Biological sensory systems work in an aqueous environment. This means that water must be included in the thermodynamic considerations. Referring back to Fig. 2.2, you can see the water molecules (gray spheres) interact (hydration) with both **S** and **X**. This is because the hydrogen bond, ion–dipole, and dipole–dipole interactions exhibited by  $\text{H}_2\text{O}$  have enough energy to cause such association. When **S** and **X** are separated (Fig. 2.2b), there are arbitrarily selected two free (random) molecules of water present in the system.

For a unique description of the system we have to specify the coordinates of all the components. If we place the origin of the coordinate system in the binding site **S**, then the position of the remaining particles is uniquely described by  $3n = 9$  coordinates. Those are their degrees of freedom. On the other hand, when the complex **SX** is formed (Fig. 2.2c), 14 more water molecules will have been liberated from the cleft. This increases the number of the particles to 15 and the number of degrees of freedom to  $15 \times 3 = 45$  (the numbers correspond, of course, to Fig. 2.2, but are otherwise arbitrary). This increase of degrees of freedom results in the increase of the entropy (and a corresponding reduction in the free energy) of the whole system. Thus, the binding free energy is driven by the entropy of hydration. Its equivalent enthalpy value/interaction is included in Table 2.1 for comparison.

For the purpose of this discussion, it is most important to realize that the hydrophobic bond will contribute to the free energy of interaction only if the two molecules geometrically fit and eliminate some hydration water from the binding cleft and its vicinity. It is this condition that primarily accounts for the high selectivity found in the immunochemical reactions, biological receptor binding, enzyme/substrate recognition, and so on. It is also combined with enthalpy-driven binding, which can again act only at a relatively short range.

The equilibrium constants of some biological recognition reactions have a stronger dependence on temperature than others, implying that the relative contribution to free energy change from, for example, the hydrogen bond (enthalpy) and the hydrophobic bond varies (Absolom and van Oss, 1986). The important corollary for the design of so-called biosensors is that it would be difficult to employ a water-based biological selective system (e.g., most enzymes or antibodies) for water-free applications.

### 2.2.2 Bioselectivity

Specific binding sites of biological origin define a special class of chemical sensors: biosensors. Due to their exceptionally high selectivity, these bioligands have been the subject of intense interest among sensor scientists and engineers. They are classified in Table 2.2.

Unfortunately, high selectivity implies strong binding energies, often in excess of  $100\text{ kJ mol}^{-1}$ . It then becomes a case of “too much of a good thing.” Once again, we must invoke the difference between the sensor and sensing system (or assay). The latter requires some intervention in order to disassociate the strong complex formed

**Table 2.2** Bioligands used in biosensors and bioassays

Bioligand	Use
Antibodies/antigens	Immunoassays
Oligonucleotides	DNA (RNA) bioassays
Aptamers	Bioassays
Enzymes	Enzyme sensors
Receptors	Bioassays
Cells and tissues	Bioassays

between the biological ligand and the substrate. Such a step places them outside the definition of the chemical sensors and outside the scope of this book. However, they are briefly discussed here for several reasons.

First, it may help to clarify the misuse of the term “biosensor.” Perhaps more important, there is a real hope that these bioligands could be used in genuine biosensors if their high binding constant could be lowered to the level where they could be used in an equilibrium-binding regime. Such de-tuning of binding is possible, in principle, if the binding region in the biomolecule is covalently modified. Another possibility is to operate them under such conditions that the binding interaction is weakened to the point that equilibrium condition is established. This can be done by modifying the reaction medium, that is, increasing ionic strength and lowering the pH (immunochemical interactions), addition of “hydrogen bond breakers” (DNA, RNA binding), elevating the temperature (DNA, RNA binding), or use of mixed organic/aqueous solvents (immunochemical and receptor binding). Such a change of operating conditions may, however, impose unacceptable constraints on the operation of the biosensor. Finally, their very successful use in various bioassays is another reason for having them briefly discussed. This assessment applies to all bioligands except enzymes. They stand apart and are discussed in the section on kinetic selectivity (Section 2.3).

### 2.2.2.1 Immunochemical Selectivity

If one were to define the ideal building blocks for the construction of a selective layer, antibodies would have to be considered very seriously. Their selectivity is based on stereospecificity of the binding site for the antigenic determinant (antigen, hapten, epitope). Their production is relatively inexpensive and universal, which means that an antibody for any antigen, regardless of its shape or chemical nature, can be produced by the same general procedure. The only limitation seems to be that of the size: antigens of a molecular weight of less than 2,000 D normally do not induce an immunochemical response in B lymphocytes that produce them. In order to obtain antibodies for low molecular weight antigens (haptens) it is necessary to link the latter to a high molecular weight polymeric carrier (e.g., bovine serum albumin [BSA], polyethylene glycol, etc.).

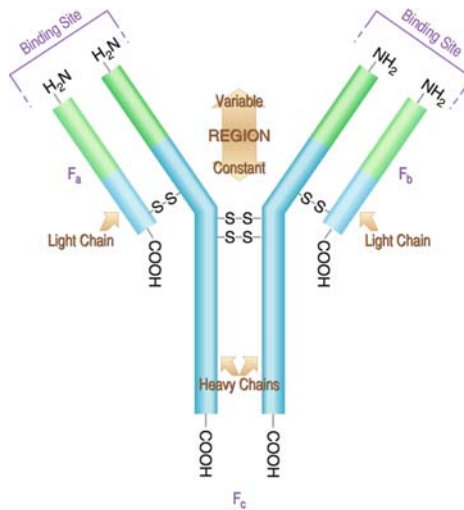


**Fig. 2.3** Schematic of antibody immunoglobulin G (IgG). It is a bivalent bioligand with binding sites formed by light-chain fragments  $F_{ab}$

Antibodies belong to the group of serum proteins called immunoglobulins (Janeway et al., 2004). Their molecular weight ranges from 140 to 970 kD. The number of antigens that can be bound to one antibody determines their valency, which is typically 2 but can be as high as 10 for immunoglobulin M (IgM). Their primary function is to disable foreign (high molecular weight) immunogens, be it proteins, nucleic acids, viruses, and so on that may invade and endanger the organism. In that respect, they can be looked at as highly specific complexing agents, which are one of the key factors in the defense mechanism. The most common antibody is immunoglobulin G (IgG) which has a molecular weight of 146,000 D and valency of 2 (Fig. 2.3). Traditionally, it has been produced by multiple sensitization (inoculation) of an experimental animal (e.g., rabbit, goat, dog, etc.) to a suitable antigen. When the natural immune response triggers the production of IgG, which is targeted against the immunogen, the specific antibody can be isolated from the animal antiserum and purified to the desired level. Antibodies produced by this procedure are called polyclonal. A more efficient procedure involves fusion of the sensitized B lymphocytes with myeloma cells (malignant cancer cells), which are then implanted in the animal. They produce large amounts of specific monoclonal antibodies, which are again harvested and purified.

Although the active site on the antibody is fundamentally highly specific to the given antigen, any preparation of antibodies (either poly- or monoclonal) is heterogeneous. This heterogeneity is far greater in polyclonal antibodies than in their monoclonal counterparts. The average ability to complex antigen is called the avidity of the preparation, and the binding equilibrium between an antibody (Ab) and an antigen (Ag) is referred to as affinity.



The binding constant  $K$  is again defined as the ratio of the forward ( $k_f$ ) and reverse ( $k_r$ ) rate constants (2.2). It ranges from  $K < 10^4 \text{ L M}^{-1}$  for weak binding of antigens of MW  $< 2,500 \text{ D}$  to  $K > 10^9 \text{ L M}^{-1}$  for antigens of MW  $> 6-8 \cdot 10^6 \text{ D}$ , which are very strongly bound.

Under physiological conditions, an equilibrium constant in the range of  $K = 10^5$  to  $10^9 \text{ L mol}^{-1}$  corresponds to a  $\Delta G^0$  range of  $-25$  to  $-50 \text{ kJ mol}^{-1}$ . The forward rate of the immunochemical reaction is invariably very high (diffusion-limited). This is consistent with the strategy of the biological defense mechanism, where the inactivation of a “potentially harmful” antigen must be done with maximum speed, but the recognition of the truly harmful (or innocuous) constituent can be done much more slowly. This means that the dissociation rate constants vary over 7 decades from  $10^{-4} \text{ s}^{-1}$  to  $10^3 \text{ s}^{-1}$  and determine the overall high affinity of the hapten or antigen to the antibody.

The nature of the Ab–Ag bond is of critical importance for analytical purposes. The most prevalent bonds are considered to be Coulombic and van der Waals interactions. The role of water in the overall binding is also critically important. First of all, it is the prerequisite in the formation of the hydrophobic bond. However, expulsion of water from the binding site, which takes place during binding, decreases the local dielectric constant and increases the strength of the Coulombic and van der Waals bonds (Table 2.1) in that region. Thus, the binding is cooperative. The close stereospecific fit is, of course, necessary. There is no covalent bonding involved in any immunochemical reactions.

The binding equilibrium expressed as shown above (2.2) is actually a gross oversimplification of the situation. The heterogeneity of the binding sites and multiple valency of individual antibodies lead to formation of secondary bonds that contribute to hysteresis or “ripening” of the antibody–antigen complex. Its ultimate form is the polymerization of a primary complex, which happens when the antigen is also polyvalent. Formation of the polymer (precipitin reaction) renders such a reaction virtually irreversible.

The secondary bonds, which may be formed much more slowly than the primary bonds, actually contribute more to the overall affinity. For example, the primary (Coulombic) bond between bovine serum albumin (BSA) and anti-BSA IgG is  $3.3 \text{ kcal M}^{-1}$  whereas the secondary bond (van der Waals) is  $28 \text{ kJ}$ , for a total  $\Delta H = 42 \text{ kJ}$ . Because the formation of the secondary bond is much slower, it is easier to prevent formation of the strong complex rather than to try to dissociate it. This is one reason why the competitive immunoassays yield results that correlate with the equilibrium-binding constants, but any such direct-binding assays have to rely on the measurement of the initial rate of binding.

In order to assess the utility of the immunochemical reaction for chemical sensing, we need to examine the effects of the experimental conditions on the primary association reaction. The effect of temperature is not particularly distinct for most reactions and cannot be generalized. This is due to the fact that the relative



contribution of the hydrophobic (entropic) bond and other (enthalpic) bonds is different. The equilibrium is largely insensitive to pH (between 6.5 and 8.5) and normal ionic strength. However, lowering the pH below 2 and increasing the ionic strength above 1 M weakens the Ab\*Ag complex to the point that it can be dissociated. The presence of organic solvents begins to play a role only when the hydrophobic bonds become affected. Obviously, the presence of water in the binding process is mandatory.

The dissociation of the “aged” immunochemical complex can be achieved, but sometimes only under denaturing conditions. The techniques that have been used mainly for preparative purposes include use of chaotropic salts (e.g., KCNS, tetraethylammonium chloride, guanidine hydrochloride, etc.). These salts compete for “available” water. Ionic (sodium dodecyl sulfate) and nonionic (polyethyleneglycol) detergents as well as solvents (ethanol, dimethyl sulfoxide) play a similar role. In general, these agents tend to disrupt the hydrophobic bond and have to be applied in relatively high ( $\sim$ M) concentrations. Disruption of hydrogen bonds (which leads to denaturation in most cases) is done by addition of 6–8 M urea and/or by lowering the pH to approximately 2. It has been possible to dissociate the charged antigen by placing the complex in a high electric field. This is so-called electrophoretic dissociation, which works only in solutions of very low ionic strength. Finally, it is sometimes possible to use low molecular weight haptens, particularly in the early stages of complex formation. In that sense the dissociation with the help of hapten can be regarded as a competitive binding.

Are antigens really the ideal binding sites for sensor applications? The answer to this question is not straightforward. First of all, the high (and time-variable) value of the affinity binding constant of particularly polyclonal antibodies makes the interaction virtually irreversible. We have to combine this with the fact that the IgG molecule is large, and that the area occupied at the sensor surface by one active site is also very large. This means that the packing density is very low and the dynamic range is narrow. This situation can be somewhat improved by isolating the binding sites from the rest of the molecule. Furthermore, we have to eliminate the multivalency in order to prevent polymerization. Again, this can be achieved at the level of a single  $F_{ab}$  fragment, as shown in Fig. 2.3. The cost of preparing single  $F_{ab}$  fragments is, however, much higher. A good strategy for improving the dynamic range would be to increase the number of binding sites by immobilizing them in a layer, rather than on the surface, and to incorporate sites with widely different values of the binding constant. The formation of the secondary bonds should be prevented. There is no simple recipe for doing this, except a mode of operation resembling competitive binding.

In contrast with sensors, sensing systems are ideal for exploitation of immunochemical selectivity. This accounts for various highly sensitive and successful competitive immunoassays. Incorporation of the manipulative step(s) opens the door for regeneration of the antibody or even for operation under virtually reversible conditions.

### 2.2.2.2 Nucleotide-Based Selectivity

The selectivity of DNA (and RNA) interaction is probably the highest of all biological recognition sites. It is unique in that it relies exclusively on highly stereospecific hydrogen bonding between base pairs: adenine–thymine and cytosine–guanine (Fig. 2.4). The enthalpic value of one base pair formation is  $\Delta H = 20.1 \text{ kJ mol}^{-1}$  for the A–T and  $\Delta H = 57.5 \text{ kJ mol}^{-1}$  for the G–C. Because the interaction enthalpies are additive, the overall DNA fragment increases with the number of base pairs, reaching the “reversible” threshold even for a dimer. The sensing dilemma is obvious: the interaction is again too strong. The sensing reversibility can be achieved, in principle, by operating the sensor near the “melting temperature” of the duplex, but the melting point depends on the number and type of base pairs and is not generally known a priori.

It is necessary to invoke the meaning of selectivity at this point. If the DNA fragment contains a “mismatch,” it must be considered to be an interferant, or impurity, in the sensing context. However, one such mismatch may lower the interaction

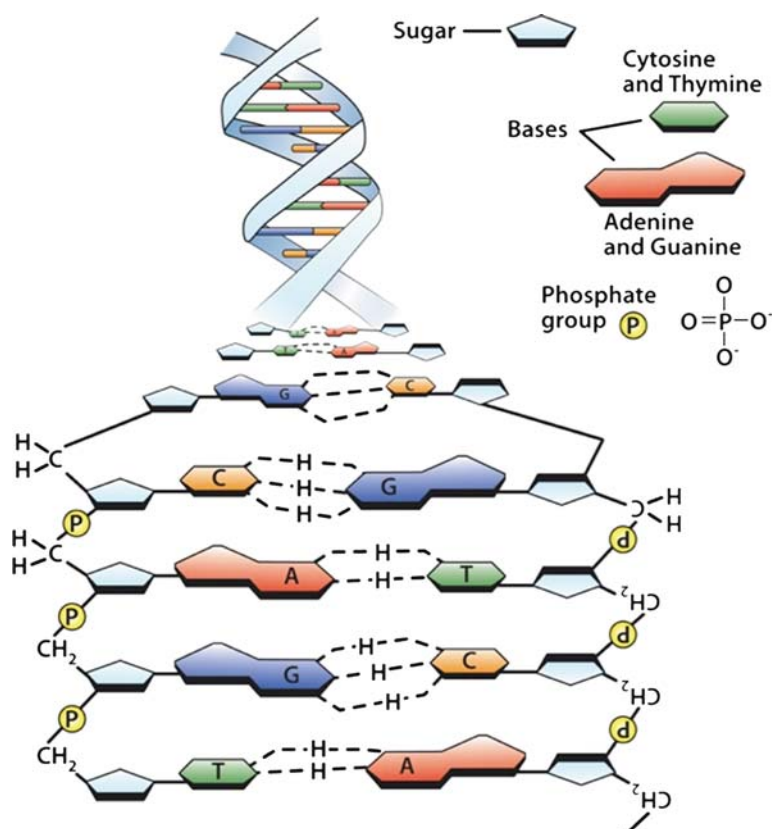


**Fig. 2.4** Hydrogen bonds in DNA base pairings

energy by such a small amount that for all purposes the binding and sensing still take place. If the transduction mechanism cannot distinguish such an event, then the advantage of high selectivity is lost. Thus, paradoxically, the high selectivity of the elementary sensing interaction becomes self-defeating. Moreover, the position of the mismatch in the DNA duplex also plays a role. The hybridization process is sequential in nature. This means that the association process starts at one end of the single strand (ssDNA) and progresses down the chain. This is known as the “kiss-and-zip” mechanism. A single mismatch is always skipped and does not play a major role in the overall result, except for a slightly lower overall binding energy and melting temperature.

### 2.2.2.3 Aptamers

These are “artificial/natural” oligonucleotides (DNA or RNA), in which the principle of the biological “lock-and-key” recognition is preserved (Fig. 2.5a).

They are capable of binding small molecules in the range of 100–10,000 D. They have been designed for assays of drugs, small proteins, and other small molecules (Tombelli et al., 2005). Their affinity is comparable to, or higher than, corresponding monoclonal antibodies. It is due to the unique folding ability of RNA and of single-stranded DNA. They are prepared by an entirely in vitro procedure called

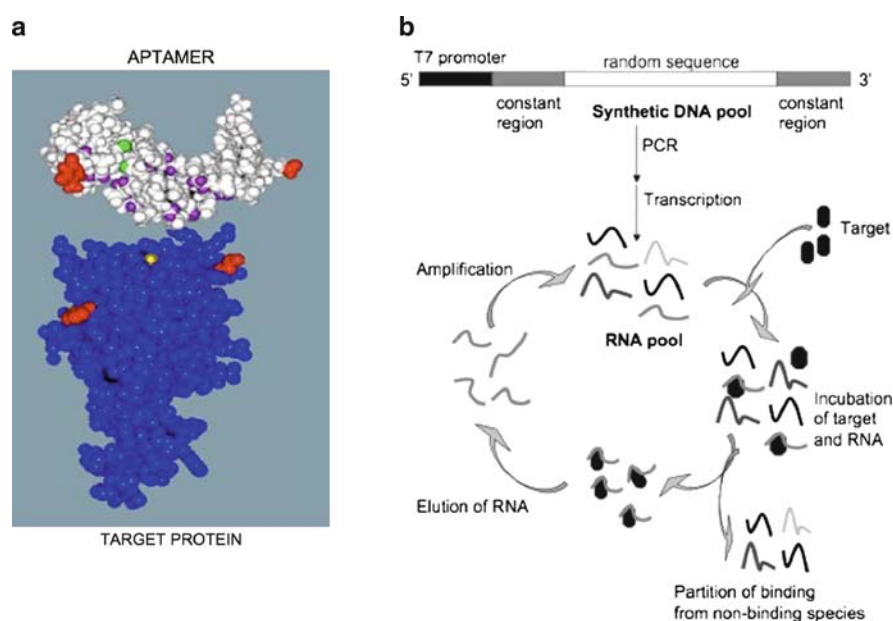


**Fig. 2.5** (a) An aptamer-target protein interaction (adapted from Tuerk and Gold 1990, p. 505). (b) Principle of the Systematic Evolution of Ligands by Exponential Enrichment (SELEX) process (adapted from Tombelli et al., 2005, p. 2424)

the SELEX (Systematic Evolution of Ligands by Exponential Enrichment) process (Tuerk and Gold, 1990; Fig. 2.5b). It is obvious that they suffer from the same problem as other bioligands with a high binding constant, that is, a virtual irreversibility. There are a number of applications in bioassays (Tombelli et al., 2005) where they show better performance (namely long-term stability) than antibodies. What makes them potentially interesting for reversible sensing applications is the opportunity to manipulate, specifically to *decrease*, the binding constant to the point that they would operate in the reversible regime.

### 2.2.3 Imprinted Polymers

Another way to realize the shape recognition ability is through the process known as “molecular imprinting” (Diaz-Garcia and Badia, 2004; Haupt, 2004). The process is depicted in Fig. 2.6.

In this process, a template molecule creates a “footprint” in the polymerizing matrix. After its removal from the polymerized material this footprint becomes a shape-recognizing specific binding site for the same molecule. The idea of molecular imprinting is quite old, dating to the mid-1950s when Linus Pauling reported selective sorbents from silica gels. Imprinted polymers came later and have been successful as stationary phases in chromatographic separations, particularly of chiral isomers. In applications as direct sensing materials, however, their success has been quite limited.

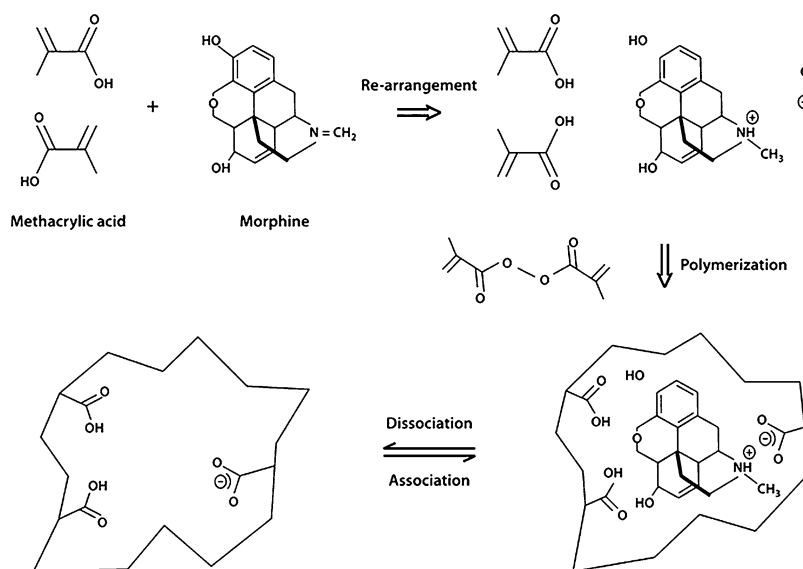


**Fig. 2.6** Principle of molecular imprinting (adapted from Diaz-Garcia et al., 2004)

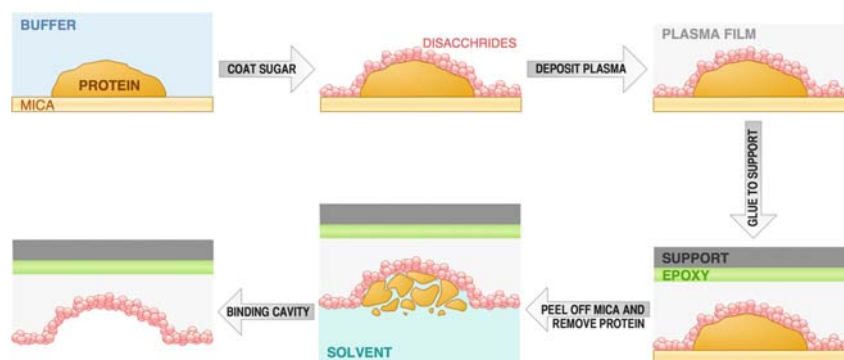


**Fig. 2.7** Creation of an "imprinted" surface

There are two processes by which the bulk imprinted polymers are formed: covalent imprinting and noncovalent imprinting. In the former, the template molecule is first covalently functionalized with the monomer, and then copolymerized with the pure monomer. After that the covalent bond is broken and the template molecule is removed by extraction. In order to facilitate the extraction step, a so-called porogenic solvent is used. It effectively swells the polymer matrix.

In the noncovalent approach, the monomer is self-assembled around the templating molecule and then again copolymerized with the additional monomer. The template is then removed by using a porogenic solvent.

It is also possible to prepare molecularly imprinted surfaces (Huaiqiu Shi et al., 1999). The process is depicted in Fig. 2.7. First the template (in this case protein) is deposited on a mica surface, which is atomically smooth. Next, the surface and the adsorbed protein are coated with water-soluble disaccharide (sugar). After that, a fluoropolymer is deposited by plasma polymerization of  $C_3F_6$ . A mechanical support is then added by attaching a glass coverslip with epoxy. Finally, the mica support is peeled off and the sugar coating and protein molecules are washed away, exposing the "footprint pit" where the protein was. The thus-prepared surface shows up to a tenfold preferential enhancement of adsorption of the template protein molecule as compared to other nonimprinted proteins.

There are several reasons why imprinted polymers do not match the affinities of natural stereospecific binding sites. First of all, the shape alone (i.e., entropic contribution) is not sufficient. The specific short-range interactions that exist in the natural binding sites generally do not exist in the imprints. Second, it is implicit in solution polymerization that the templating molecules and the monomers are solvated and that the solvation shell contributes to the overall shape and size of the template in a significant way. When the imprinted material is used in a solid-gas interaction, the fit of the molecule without the solvent is poor. Another reason is that a "tight fit" implies that the template is locked in the bulk of the polymer matrix and cannot be extracted, even with the aid of the porogenic solvent. The fact that it is leached out and that the template molecule can exchange between the imprint and the sample is because the fit is not as good as it has been expected. Therefore,

the binding reversibility and the stereoscopic specificity are two conflicting requirements. This problem does not exist on the imprinted surface, where the binding pit is freely accessible. Only properly designed baseline experiments can truly assess the viability of the imprinting approach.

### 2.2.3.1 Solubility in Organic Materials

The main difference between the materials described in this section and the previous ones is that these materials are homogeneous. In other words, there are no discrete binding sites and the interaction between the analyte and the selective layer is governed by the Gibbs equation (see (2.1)). The solid phase is treated as a solid solvent to which the analyte partitions from the sample. The solid phase can be amorphous or polycrystalline or even a gel and the sample can be liquid or gas. An immediate analogy comes to mind: a gas chromatographic (GC) experiment. There, the sample partitions between the mobile gas or liquid phase and the stationary, solid, or semiliquid phase. Indeed, such an analogy leads to one of the most successful empirical relationships, the Linear Solvation Energy Relationship (LSER) that has been used in the design of selective layers, particularly for gas sensing. The partitioning process is described by (2.3).

$$\Delta G_S^0 = -RT \ln K_S = c + rR_2 + s\pi_2 + a\Sigma\alpha_2^H + b\Sigma\beta_2^H + l\log(^{16}L) \quad (2.3)$$

The lower-case coefficients are related to the sorbent material and the capital and the Greek letters describe the gas. Hundreds of these values have been compiled and tabulated from the GC data (Abraham, 1993).

The terms on the right-hand side of (2.3) have the meaning of individual contributions to the Gibbs free energy change according to specific interactions, more or less matching those given in Table 2.1. The second term,  $rR_2$ , is the polarizability, which describes the interactions involving induced dipoles. The term  $s\pi_2$  is the polarity, describing ion–dipole and dipole–dipole interactions. The terms  $a\Sigma\alpha_2^H$  and  $b\Sigma\beta_2^H$  relate to hydrogen bonding at acidic ( $a$ ) and basic ( $b$ ) sites, respectively. Finally, the last term ( $l\log(^{16}L)$ ) is related to the dispersion of van der Waals interactions. The superscript 16 indicates the carbon-16 alkyl chain against which the dispersion has been referenced.

The usefulness of the LSER approach hinges on the similarity of the partitioning coefficients obtained from the sensing experiments ( $K_S$ ) and the gas chromatographic experiments ( $K_{GC}$ ). In other words, it is assumed that the relationship  $K_S \approx K_{GC}$  holds. This is how LSER is used for evaluation of a new sensing material. First, the coefficient  $K_{GC}$  is obtained from the tabulated database or experimentally. Second, the multiple linear regression technique (see Chapter 10) is used to obtain the best fit for the sensor test data, and the individual coefficients in (2.3) are evaluated. This approach has been used successfully in evaluation of multiple materials for gas sensors (Abraham et al., 1995; Grate et al., 1996).

The coefficient  $c$  in (2.3) is a fitting parameter; it does not have an assigned physical meaning, but may account for the difference between the static ( $K_S$ ) and dynamic ( $K_{GC}$ ) nature of the two experiments. It has been found that the GC partitioning coefficients are consistently lower by a factor  $\sim 4$ , than those obtained from the mass sensor measurements with QCM and SAW sensors (Chapter 4; Hierlemann et al., 2001). This discrepancy may have its origin in the different nature of the two experiments. In the chromatographic experiment, the gas molecules at the front of the advancing zone encounter “pristine” sorbent material. This is particularly important when a mixture of analytes is evaluated. Second, the GC measurement is dynamic and not done under the conditions of fully developed equilibrium. Nevertheless, in spite of this discrepancy, the predictive properties of LSER have been exceptionally successful in the design of new sensing materials. The main domain of LSER application has been in the design of selective layers for various types of mass sensors.

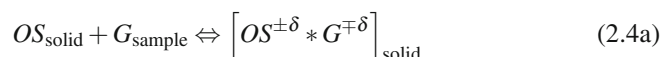
One type of interaction that is not covered in the LSER equation (2.3) is formation of the charge-transfer complex, which can also increase the solubility of the gas on the selective matrix. Partial transfer of charge in electron donor–acceptor interactions is a common notion in organic chemistry (Reichardt, 1988). The bond that is formed is a dipole whose dipole moment depends on the fraction of transferred charge ( $\delta$ ), and on the separation distance. When this interaction takes place between two molecules, the positive end of the dipole ( $\delta^+$ ) is located at the donor molecule and the negative ( $\delta^-$ ) at the acceptor molecule. The amount of transferred charge depends on the electron affinities of the participating molecules. The notion of electron affinity applies also to electronically conducting solid phases where it is related to the position of the Fermi level and the value of work function (Appendix D). If the material has a high value of work function it will act as an electron acceptor and vice versa. Therefore, molecules of gas that have low electron affinity (i.e., low ionization potential) will partially transfer electrons to the conduction energy band of the material and become associated with the matrix. From the material’s point of view, this guest–host interaction represents a form of doping that changes the electronic properties of the material, namely its conductivity and work function. From the guest molecule viewpoint, it increases its solubility in the matrix. The geometrical arrangement of this association is highly specific to the material.

It is important to realize the crucial difference between charge-transfer doping and ionization doping. In charge-transfer doping, it is the electrically neutral molecule that interacts with the solid matrix. Such an interaction is typical for gases and can be exploited in gas sensors. On the other hand, in the ionization doping process, the electron is completely exchanged between the guest molecule and the matrix, leaving the usually immobile donor cation (in n-doping) or immobile acceptor anion (in p-doping). In chemists’ language, the charge-transfer doping process constitutes Lewis acid–base chemistry whereas the ionization doping is characteristic of the ionization or oxidation-reduction (redox) process. This distinction is critically important for chemical sensing. The ionization doping is the key mechanism of ion-selective electrodes (Chapter 6) where the ion selectively partitions into the organic phase, called the ion-selective membrane. On the other hand,

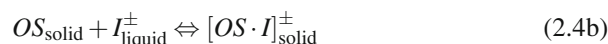


charge-transfer doping is the key mechanism in work function sensors (Chapter 7; Janata and Josowicz, 1998). The transduction principles that apply to these two interactions are substantially different. The two mechanisms can be represented as follows.

Charge-transfer doping:



Ionization doping:



The asterisk in (2.4a) indicates that the guest molecule  $G$  is associated with the organic semiconductor (OS) in some intimate, dipolar geometrical arrangement dictated by the partially exchanged charge  $\delta$ . Because the guest molecule is electrically neutral, the sample from which this molecule can be partitioned can be either gas or liquid. However, partitioning of ions applies to partitioning between OS and a liquid sample. The organic materials that fall into this category of selective materials are all organic semiconductors, namely conducting polymers, redox polymers, and van der Waals organic solids (Janata and Josowicz, 1998). Because there are many more electrically neutral gases to be detected than ions, the charge-transfer doping is potentially the more prevalent type of interaction.

It was mentioned at the beginning of this section that the distinguishing feature of materials based on solubility-based selectivity is that they are homogeneous. However, this statement should not be taken too literally, because enhancement of selectivity can be achieved by incorporating specific binding sites into these matrices. The choice of correct transduction mechanism then depends on the type of analyte/selective layer interaction. Generally speaking, detection of mass change will work in all modes of solubility-based selective materials, as long as the mechanical properties of such layers are not affected (Hierlemann et al., 2001; Topart and Josowicz, 1992).

### 2.2.3.2 Solubility in Inorganic Materials

Although the general principle of partitioning equilibrium remains the same, there are additional mechanisms, and the underlying physical principles governing inorganic materials are different. An important, albeit somewhat unique, example is the solubility of hydrogen in palladium metal in which the charge-transfer mechanism again applies. Molecular hydrogen first dissociates into atomic hydrogen (Ekedahl et al., 1998), which then diffuses into the Pd bulk, forming bulk palladium hydride  $\text{PdH}_x$  (Fig. 2.8).

Thus, at the surface



This is followed by





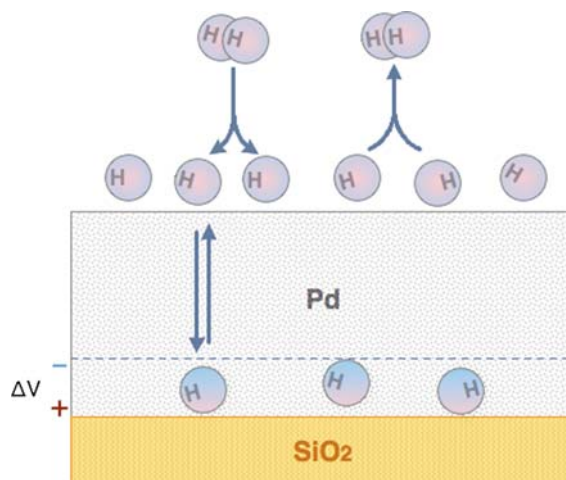


**Fig. 2.8** Palladium/hydrogen interaction

In the absence of oxygen, the reaction depicted by (2.5) is reversible. However, when oxygen is present, a competing oxidation takes place at the Pd surface, making the overall reaction irreversible.



Hydrogen is a very important species and various hydrogen sensors based on reactions (2.5) through (2.7) have been commercialized. They are discussed in more detail later.

An entirely different selectivity principle known as phase equilibrium comes into play in high-temperature ionic conductors. Many important gases dissolve in ionic solids at elevated temperatures. However, the solubility is rather sharply defined for the gas and the solid by the lattice parameters and the size of the gas molecule. The best example is the solubility of oxygen in zirconium dioxide. When  $\text{ZrO}_2$  is doped with yttrium ions, it exhibits a high mobility for the  $\text{O}^-$  anion. The solubility and anion mobility then become the basis for several electrochemical gas sensors, using “yttria-stabilized zirconia” (YSZ).

There are several factors that make solid-state ionic conductors attractive for chemical sensing purposes. One is the aforementioned selectivity stemming from the narrowly defined solubility. Second is the fact that these materials are intensively investigated as building blocks of fuel cells and the knowledge database (useful also for sensors) is rapidly expanding. Third is their operating temperature, which is typically well above the boiling point of water, eliminating this ubiquitous interference so often found in room-temperature sensors. (The reverse side of this coin is that the high temperature requirement somewhat limits their applications.) Finally, the diffusion is faster at higher temperatures, resulting in faster response time.

## 2.3 Kinetic Selectivity

This form of selectivity applies to sensors that operate in the steady-state regime. The prime examples are thermal and amperometric sensors. It is somewhat limited for potentiometric sensors and it is least suitable for mass sensors. The minimum necessary kinetic background information can be found in Appendix B.

Consider a mixture of species,  $X_1, X_2, \dots, X_n$ , which are undergoing common chemical transformation to products P, but with different reaction rates.



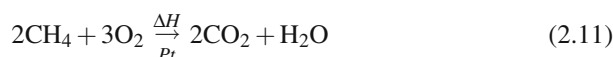
Let us assume that a catalyst can selectively increase the rate of conversion of the analyte  $X_X$ .



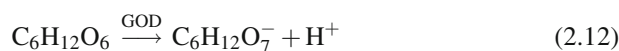
Therefore,

$$k_X \gg k_1, k_2, \dots, k_n \quad (2.10)$$

Such a situation may arise, for example, in the combustion sensor in which the species of interest is methane and the other combustibles are different higher molecular weight hydrocarbons. The catalyst, in this case, can be Pt and the preferentially catalyzed reaction is as follows.



This is the reaction taking place at the surface of the thermal sensor, the pellistor, discussed in Chapter 3. An example of a biocatalyst is the enzyme glucose oxidase (GOD) which highly selectively promotes oxidation of D-glucose to gluconic acid.



This reaction is used throughout this book because it is the most common biocatalyst in the biosensor literature and it is discussed in greater detail below.

### 2.3.1 Enzyme Kinetics

In terms of sensing applications, enzymes vastly outnumber any other type of catalysts. They are natural products in biological systems where their primary function is to control the rates of important reactions, mainly, but not exclusively, in metabolism. There are a few lipophilic enzymes, but for the most part they function

in an aqueous environment. Enzymes are the key component in the largest group of biosensors. In the following section we outline the fundamentals of enzyme kinetics. The specific differences that arise from the different transduction mechanisms of different sensors are discussed separately. Here, we focus only on the key aspects of enzymatic reactions.

Enzymes are a special kind of catalyst, proteins of MW 6,000–400,000 which are found in living matter. They have two remarkable properties: (1) they are extremely selective to the given substrate; and (2) they are extraordinarily effective in increasing the rates of reactions. Thus, they combine the recognition and amplification steps. A general, enzymatically catalyzed reaction can be described by the Michaelis–Menten mechanism, in which E is the enzyme, S is the substrate, and P is the product, formed from the intermediate complex ES.



The reaction velocity ( $v$ ) can be expressed as the rate of increase of the concentration of the product P.

$$v = \frac{dC_P}{dt} = k_2 C_{ES} \quad (2.14)$$

For a high value of substrate concentration, the reaction velocity reaches its maximum (saturation). Under those conditions, all the available enzyme  $E_T$  is bound in the complex with the substrate. Thus

$$v_{\max} = k_2 C_{E_T} \quad (2.15)$$

This means that the maximum velocity is proportional to the concentration of the enzyme. Below saturation, the enzyme is present either in free form or complexed with the substrate.

$$C_{E_T} = C_E + C_{ES} \quad (2.16)$$

At steady state, the concentration of the ES complex is constant.

$$\frac{dC_{ES}}{dt} = k_1 C_S C_E - (k_{-1} + k_2) C_{ES} = 0 \quad (2.17)$$

The Michaelis–Menten constant ( $K_m$ ) is defined as

$$K_m = \frac{k_{-1} + k_2}{k_1} = \frac{C_S C_E}{C_{ES}} \quad (2.18)$$

Substitution for  $C_E$  from (2.16) into (2.18) yields

$$K_m = \frac{C_S (C_{E_T} - C_{ES})}{C_{ES}} \quad (2.19)$$

This, when combined with (2.14) and (2.15), gives

$$K_m = \frac{C_S(v_{\max} - v)}{v} \quad (2.20)$$

After rearrangement, we obtain the Michaelis–Menten equation.

$$v = \frac{v_{\max} C_S}{C_S + K_m} \quad (2.21)$$

It can be shown that  $K_m$  equals the concentration of the substrate at which the reaction velocity is one half of its maximum. The Michaelis–Menten constant is an important figure of merit for the enzyme. It is the measure of its activity. Although it describes a kinetic process, it has the physical meaning of dissociation constant, that is, a reciprocal binding constant. It means that the smaller the  $K_m$  is, the more strongly the substrate binds to the enzyme.

The extraordinary specificity of enzymatic catalysis is due to the shape recognition. Enzymes are proteins having a stereospecific binding site. At this site, the two reactants (in the above example, D-glucose and oxygen) are brought together in a precise and favorable orientation for the reaction to take place.

As with any other proteins, enzymes are subject to acid–base equilibria that affect their catalytic properties, that is, their  $K_m$  value. Each enzyme has its own characteristic pH dependence  $\mathfrak{R}_{\text{pH}}$ . Thus, the general Michaelis–Menten equation, which takes into account this pH dependence of  $K_m$ , can be written as in (2.22).

$$v = \mathfrak{R}_{\text{pH}} \frac{v_{\max} C_S}{C_S + K_m} \quad (2.22)$$

In addition to hydrogen ions, other species can also affect the enzymatic catalytic activity. This phenomenon is called inhibition; it may be specific, nonspecific, reversible, or irreversible. The inhibition reactions can also be used for the sensing of inhibitors. The best-known example is the sensor for detection of nerve gases. These compounds inhibit the hydrolysis of the acetylcholine ester which is catalyzed by the enzyme acetylcholine esterase. Acetylcholine ester is a key component in the neurotransmission mechanism.

Enzymatic reactions combine substrate specificity with a high amplification factor. From that viewpoint they are ideal selective layers for chemical sensors. However, they are not specifically part of the information acquisition/processing scheme in nature. Their exclusive role is to lower, highly selectively, the activation energy barrier of certain reactions, thus acting as regulators. A general diagram of an enzymatically coupled chemical sensor is shown in Fig. 2.9.

The geometry shown here corresponds to a semi-infinite planar diffusion. Other geometries (e.g., radial geometries) typical for microsensors can be used. The enzyme-containing layer is usually a hydrogel, whose optimum thickness depends on the enzymatic reaction, on the operating pH, and on the activity of the enzyme (i.e., on the  $K_m$ ). Enzymes can be used with nearly any transduction principle, that is, thermal, electrochemical, or optical sensors. They are not, however, generally suitable for mass sensors, for several reasons. The most fundamental one is the fact

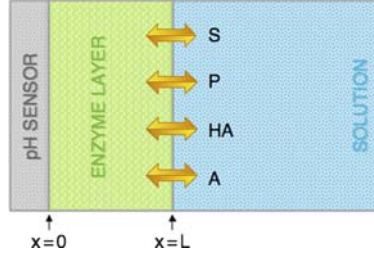


**Fig. 2.9** Zero-flux-boundary enzymatic sensor

that the net mass change in a catalyzed reaction is usually small. Moreover, the mass sensors do not perform well in a gel, due to the mechanical damping.

The basic operating principle of enzyme use in sensors is simple: an enzyme is immobilized inside a permeable layer, into which the substrate(s) diffuse and from which the product(s) can effuse. Any other species that participate in the reaction, such as buffers, must also diffuse in and out of the layer (see Fig. 2.9). Because of the combined mass transport and chemical reaction, this scheme is often referred to as the diffusion–reaction mechanism.

Mathematically, this case is described by the set of second-order partial differential equations, which are usually solved numerically. The general unidirectional (in the  $x$ -coordinate) diffusion–reaction equation for any species  $i$ , is

$$\frac{\delta C_i}{\delta t} = D_i \frac{\delta^2 C_i}{\delta x^2} \pm \Re_{\text{pH}}(C_i) \quad (2.23)$$

Here,  $t$  is time and  $x$  is the distance traveled within a layer of thickness  $L$ .  $D_i$  is the effective diffusion constant of the species  $i$ . The first term represents the mass transport, and the second is the pH-dependent “reaction term.” This equation has to be written for every participating species, with the appropriate sign in front of the reaction term.

When the pH-dependent Michaelis–Menten equation (2.22) is substituted for the pH-dependent reaction term  $\Re_{\text{pH}}(C_i)$ , we obtain for the substrate  $S$  at any point inside the enzymatic gel layer

$$\frac{\delta C_S}{\delta t} = D_S \frac{\delta^2 C_S}{\delta x^2} - \frac{\Re_{\text{pH}} v_{\text{max}} C_S}{(C_S + K_m)} \quad (2.24)$$

The first term on the right-hand side of (2.24) is the diffusion term, where  $D_S$  is the effective diffusion constant of the substrate. The second term is called the kinetic (reaction) term. It is necessary to normalize the variables as follows.

$$t = \frac{t^* L^2}{D_S} \quad (2.25a)$$

$$C_S = C_S^* K_m \quad (2.25b)$$

$$x = x^* L \quad (2.25c)$$

In (2.25a–c), the variables with the asterisk are dimensionless. Substitution into (2.24) yields a dimensionless diffusion–reaction mechanism equation.

$$\left( \frac{\delta C_S}{\delta t} \right)^* = D_S \left( \frac{\delta^2 C_S}{\delta x^2} \right)^* - \phi^2 \left( \frac{C_S}{1 + C_S} \right)^* \quad (2.26)$$

The parameter  $\phi$  is called the Thiele modulus.

$$\phi = \frac{L v_{\max}^{1/2}}{(K_m D_S \mathcal{R}_{\text{pH}})^{1/2}} \quad (2.27)$$

It contains all important design parameters, as well as the pH-dependency of the enzyme activity. It defines two operating regimes: for  $\phi > 10$ , the mechanism is diffusion-controlled, and for a Thiele modulus  $\phi < 5$ , it is reaction-controlled. In other words, it defines which of the terms on the right-hand side of (2.26) controls the rate of the conversion of the substrate. Because the terms are operating in series, the smaller of the two is dominant. For chemical sensing, diffusion control is always preferable. In order to have a high value of the Thiele modulus, we want to increase the thickness of the layer ( $L$ ), decrease the effective diffusion constant of the substrate ( $D_S$ ), and increase the enzyme loading (i.e.,  $v_{\max}$ ). The value of  $K_m$  is a given for the enzyme. However, if we have a choice, the enzyme preparation with lower  $K_m$  is preferable.

Because there are several species diffusing into and out of the gel, the normalization transformation must be done for all of them, leading to the system of second-order partial differential equations. Each species has its own Thiele modulus and again it is the smallest one that determines the overall outcome. The complicating factors are the reactions involving the buffer; these are very fast. In mathematical terms, it means that they are algebraic and the resulting partial differential equations are “stiff”, requiring numerical solution (Caras et al., 1985a). As always with the differential equations, the final solution depends on the initial conditions and on the boundary conditions. The crucial ones define the conditions at the transducer/gel interface ( $x = 0$  in Fig. 2.10). If none of the reacting species can cross this interface, the boundary is called a zero flux boundary. It is found in thermal, potentiometric, and optical sensors. However, in amperometric sensors, at least one of the species is consumed at this interface (typically oxygen), and a gradient of that species is established. The interface is then called the nonzero flux boundary. This difference in operating mechanism has a profound influence on the performance of such sensors, as we show in Chapter 7.

The boundary and initial conditions are always defined by the assumptions that have been made in the formulation of the model. These, in turn, depend

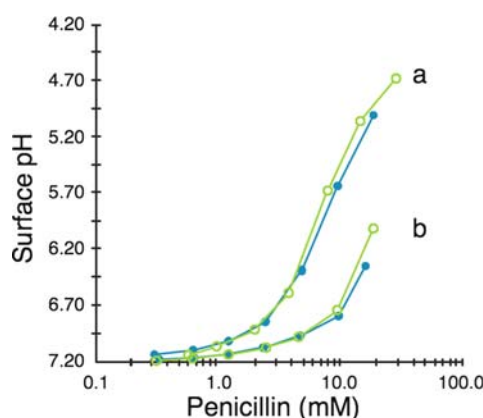


**Fig. 2.10** Effect of buffer capacity on penicillin calibration curves: (a) 20 mM phosphate buffer and (b) 80 mM phosphate buffer (adapted from Caras et al., 1985a, p. 1925)

on approximations and compromises. Let us now review briefly the approximations that have been made, more or less historically, by various enzyme sensor investigators, and rank them in the approximate order of severity.

1. There is a linear diffusion gradient inside the enzyme layer.
2. There is no pH dependence of  $K_m$ .
3. There is no effect of mobile buffer capacity.
4. There is no effect of fixed (i.e., the gel itself) buffer capacity.
5. There is no partitioning of reactants and products between the gel and the sample.
6. There is no Donnan potential at the gel/sample boundary.
7. There is no depletion layer at the gel/sample boundary.

Approximations (1) and (2) have been made in the earliest models of development of enzymatic sensors in order to simplify the mathematics. They are both bad; the concentration profiles are nonlinear (Caras et al., 1985a; Eddowes, 1985) and the pH dependence of enzyme kinetics is an established fact.

Approximations (3) and (4) would be the most serious for enzymatic sensors in which the sensor output is related to the change of pH, because for such sensors the buffer capacity would have to be low and constant. However, for sensors that use some other reactants/products besides hydrogen ion, a large excess of buffer would mitigate the effects of these assumptions. To some extent, they can be also mitigated by the experimental design, as we show later.

The partitioning of electrically neutral species (assumption 5) and electrically charged species (assumption 6) between the gel and the sample affects the algebraic part of the model. It is a serious problem for both electrically neutral species (e.g., oxygen) and charged (ionic) species. However, it can, to some extent, be mitigated by the choice of the gel matrix.

Assumption (7) pertains exclusively to the enzymatic sensors with a nonzero flux boundary, at the gel/transducer interface (i.e., amperometric sensors). It can be eliminated by decreasing the size of the sensor.

In summary, assumptions (1) and (2) are unnecessary and have been avoided in more advanced models. Assumptions (3) and (4) are unavoidable and illustrate the fundamental weakness of most enzymatic sensors, particularly those depending on detection of pH changes. Assumptions (5) and (6) can be avoided to some extent by experimental design, but should be always accounted for in the model. Assumption (7) is easily avoidable. There is another assumption that has not been mentioned, the equality of concentration and activity. As discussed in Chapter 1, that cannot always be a justifiable assumption.

With these assumptions in mind, we now complete the outline of the solution of the diffusion–reaction problem as it applies to the most difficult case, the pH-based enzymatic sensors (potentiometric or optical). We assume only that there is no depletion layer at the gel/solution boundary (7), and that there is no fixed buffer capacity (4). The objective of this exercise is to find out the optimum thickness of the gel layer that is critically important for all zero-flux-boundary sensors, as follows from (2.26).

As a rule, hydrogen ion is involved not only in the pH-dependency of the reaction term (Thiele modulus) but also as the actively participating species involved in the acid–base equilibrium of all the substrates, reaction intermediates, products, and even the gel matrix. Furthermore, enzymatic reactions are always carried out in the presence of the mobile buffer. By “mobile” we mean a weak acid or a weak base that can move in and out of the reaction layer, as opposed to the fixed buffer represented by the gel (and by the protein) itself. Thus, we have to include the normalized diffusion–reaction equations for hydrogen ion and for the buffer.

$$\frac{\delta C_{H,T}}{\delta t} = D_H \frac{\delta^2 C_H}{\delta x^2} + D_{HA} \frac{\delta^2 C_{HA}}{\delta x^2} + \frac{v_{\max} C_S}{\mathfrak{R}_{pH}(K_m + C_S)} \quad (2.28)$$

Here  $C_{H,T}$  is the total concentration of bound and unbound protons  $H$  within the enzyme layer and  $C_H$  is the concentration of protons. The term containing  $C_{HA}$  reflects the flux of the protonated buffer acid  $A$  in and out of the layer. The reaction term containing  $\mathfrak{R}_{pH}$  is a characteristic property of the given enzyme and of the substrate and is discussed later. For simplicity, we consider here a simple monoprotic buffer for which

$$K_a = \frac{C_H C_A}{C_{HA}} \quad (2.29)$$

Next, we have to define the boundary and the initial conditions. For the zero flux sensors (Fig. 2.9), the first space derivatives (i.e., fluxes) of all variables at the transducer/gel boundary (point  $x = 0$ ) are zero:

$$\{C_S(0,t)\}'_x = \{C_H(0,t)\}'_x = \{C_{HA}(0,t)\}'_x = 0 \quad (2.30)$$

On the other hand, in nonzero flux sensors the flux of at least one of the species (product or substrate) would be nonzero.

The concentrations of all species at the gel/sample boundary  $L$  are equal to the bulk values in the sample:



$$\begin{aligned}
C_S(L, t) &= C_{S, \text{bulk}} \\
C_{HA}(L, t) &= C_{HA, \text{bulk}} \\
C_H(L, t) &= C_{H, \text{bulk}} \\
C_A(L, t) &= C_{A, \text{bulk}}
\end{aligned} \tag{2.31a-d}$$

The initial conditions are:

$$\begin{aligned}
C_S(x, 0) &= 0, \text{ for } x < L \\
C_{HA}(x, 0) &= C_{HA, \text{bulk}} \\
C_H(x, 0) &= C_{H, \text{bulk}} \\
C_A(x, 0) &= C_{A, \text{bulk}}
\end{aligned} \tag{2.32a-d}$$

This means that all species except the substrate are initially present inside the enzyme layer.

This treatment leads to a system of stiff, second-order partial differential equations that can be solved numerically to yield both transient and steady-state concentration profiles within the layer (Caras et al., 1985a). Because the concentration profile changes most rapidly near the  $x = L$  boundary an ordinary finite-difference method does not yield a stable solution and is not applicable. Instead, it is necessary to transform the distance variable  $x$  into a dummy variable  $y$  using the relationship

$$y = L(1 - e^{-ax} + xe^{-a}) \tag{2.33}$$

This transformation allows for equal distribution in the  $y$ -space while concentrating the lines close to the  $x = L$  boundary. Parameter  $a$  sets the spacing of the lines. This technique is called MOL1D (Method Of Lines in 1 Dimension) and is suitable for solving parabolic and hyperbolic initial boundary value problems in one dimension.

The actual solution for both transient and steady-state response of any zero-flux-boundary sensor can be obtained by solving (2.26) through (2.33) for the appropriate boundary and initial conditions. Fitting of the experimental calibration curves (Fig. 2.10) and of the time response curves (Fig. 2.11) to the calculated ones, validates the proposed model.

Once the theoretical curves have been fitted (Figs. 2.10 and 2.11), it is possible to plot the concentration profiles of all the species included in the model and to determine the optimum thickness of the enzyme layer (Fig. 2.12). Because the Thiele modulus is the controlling parameter in the diffusion–reaction equation, it is obvious from (2.22) that the optimum thickness will depend on the other constants and functions included in the Thiele modulus. For this reason, the optimum thickness will vary from one enzyme and one kinetic scheme to another.

Another important set of observations is related to the detection limit: dynamic range and sensitivity. For the expected values of the diffusion coefficient (in the gel) of approximately  $10^{-6} \text{ cm}^2 \text{ s}^{-1}$  and substrate molecular weights about 300, the detection limit is approximately  $10^{-4} \text{ M}$ . This is due to the fact that the product of the enzymatic reaction is being removed from the membrane by diffusion at approximately the same rate as it is being supplied. The dynamic range of the sensor

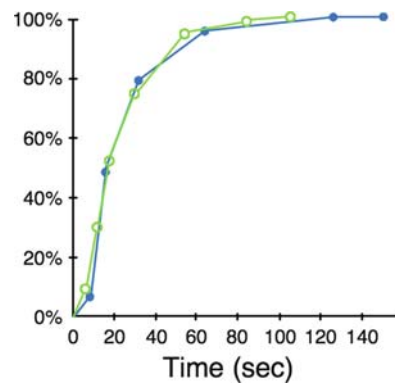


**Fig. 2.11** Theoretical and experimental time response curve for penicillin (adapted from Caras et al., 1985a, p. 1925)

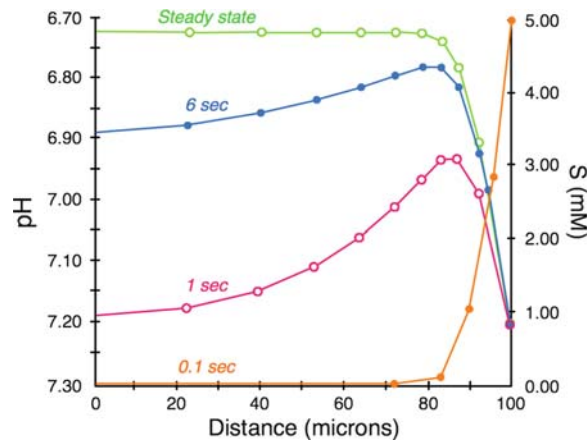


**Fig. 2.12** Calculated concentration profiles for the substrate (penicillin) and the product (hydroxium ion), expressed as pH (adapted from Caras et al., 1985a, p. 1918)

depends on the value of the  $K_m$  and on  $v_{max}$  (which depends on the enzyme loading). Generally speaking, higher loading should extend the dynamic range at the top of the concentration range. It is sometimes stated incorrectly that “the enzyme sensor has close to theoretical dependence” or a “Nernstian response,” which means that a one-decade change of the bulk concentration of the substrate is expected to yield a one-decade change at the surface ( $x = 0$ ) concentration. In the case of potentiometric enzyme sensors, it would yield a slope of approximately 60 mV/decade at 25°C. It is not intuitively obvious, but clearly evident from the comparison of the experimental and calculated response curves, that there is no general theoretical slope. Each enzymatic sensor has its own “theoretical curve,” which depends on the mechanism and on the conditions under which it operates. We must remember that the decade/decade slope would occur only if a constant fraction of the product reached the  $x = 0$  interface. The upper limit of the dynamic range depends on the value of the

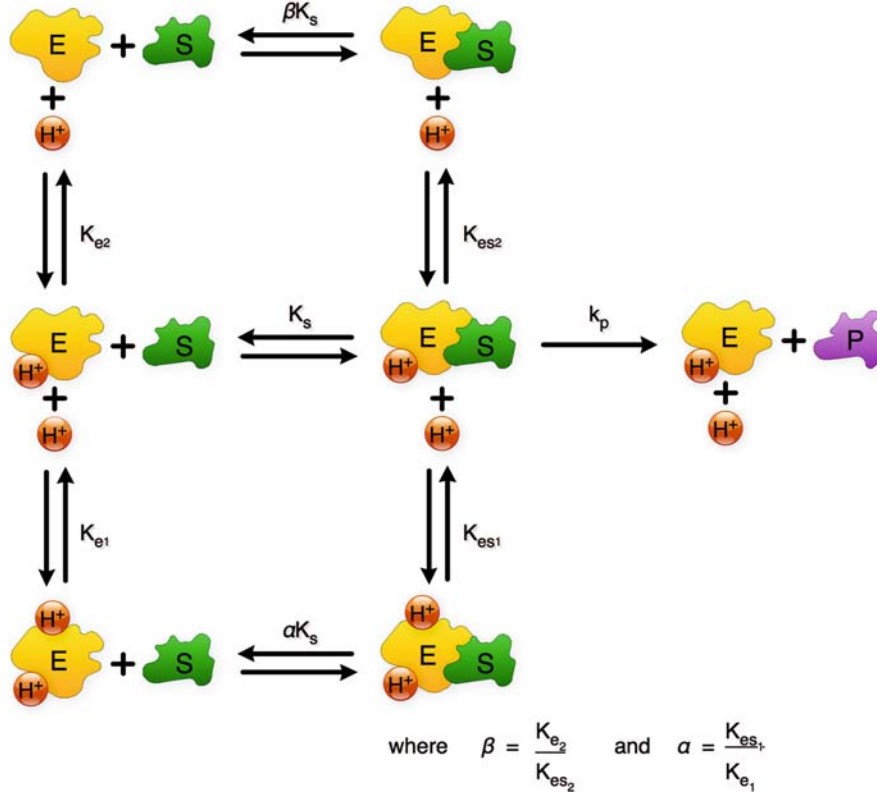


**Fig. 2.13** One-enzyme substrate scheme, including protonation equilibria

Thiele modulus. It can be increased by the enzyme loading but, obviously, only up to a point. The normal dynamic range is approximately between  $10^{-4}$  and  $10^{-1}$  M.

We now return to the dimensionless pH-dependent reaction term  $\mathfrak{R}_{pH}$  in (2.28). Enzymes are proteins that are subject to multiple protonation equilibria. In that respect, they are polyelectrolytes. The scheme shown in Fig. 2.13 depicts the simplest situation, with only one product-forming pathway in which the product **P** is formed from the protonated enzyme/substrate complex  $\mathbf{H}^+\mathbf{ES}$ .

Fractions of protonated and deprotonated enzyme are given by the dissociation equilibria, with appropriate dissociation constants. The substrate **S** shown in this scheme does not have acido-basic properties in the given pH range. Solving the equations outlined in Scheme 1 yields (for this reaction) the following relationship.

$$\mathfrak{R}_{pH} = \left( 1 + \frac{C_H}{K_{ES1}} + \frac{K_{ES2}}{C_H} \right) \quad (2.34)$$

This is the term that has to be inserted into (2.28) and normalized equations for all the other species involved in the reaction.

### 2.3.2 Zero-Flux-Boundary Sensors

Most enzyme sensor developers have used D-glucose/glucose oxidase as the first step in their studies. Glucose is an easily accessible, nontoxic substrate and D-glucose oxidase is an inexpensive and available enzyme. The reaction itself is amenable to thermal, electrochemical, and optical sensing. Blood glucose sensing is an important diagnostic problem (related to diabetes) that makes a good selling point in the perennial hunt for funding. Finally, some glucose oxidase-based sensors have been exceptionally commercially successful for specific diagnostic applications. Not surprisingly, there are thousands of glucose sensor papers in the literature. The current Internet entry “glucose sensor” netted 30,000 replies! Throughout this book, this reaction is used only for educational purposes, in order to highlight the important aspects of enzymatic sensing schemes. In no way does the inclusion of specific references imply endorsement of one or another approach.

Glucose oxidase belongs to a large and important family of enzymes that catalyze selective oxidation of various substrates. In nature, the obvious electron acceptor (oxidant) is oxygen which then becomes the second substrate in the kinetic scheme. In this form, the glucose oxidase has been used in many types of glucose sensors. Hydrogen peroxide is an intermediate in any reaction in which the oxygen is the ultimate electron acceptor. Because  $H_2O_2$  is cytotoxic, another enzyme, catalase, always accompanies the natural oxidases. Its role is to remove the  $H_2O_2$  as fast as it is formed. Nevertheless, a certain amount of hydrogen peroxide always escapes and causes damage to the parent oxidase, thus limiting its lifetime. This two-enzyme scheme is an example of an enzymatic cascade arrangement, in which the product of one enzymatic reaction (the intermediate) becomes the substrate for the next reaction. Quite often it is possible to base the sensing scheme on the interception of such an intermediate.

In spite of its importance and popularity, the fine details of the  $\beta$ -D-glucose oxidase mechanism are not completely known. The proposed model (Fig. 2.14) includes both the catalase cascade and the protonation equilibria (Caras et al., 1985b). The pH-dependent reaction term corresponding to this model is quite complex.

$$\mathfrak{R}_{pH} = \left[ \frac{1 + \frac{C_H}{K_5} + \frac{K_5'}{C_H}}{k_{cat}C_{E_{total}}} + \frac{\frac{C_H}{K_3} + 1}{k_3C_S C_{E_{total}}} + \frac{\frac{K_4}{C_H} + 1}{k_4C_{O_2} C_{E_{total}}} \right]^{-1} \quad (2.35)$$

The verification of the model is again performed by fitting the experimental calibration (Fig. 2.15) and time response (Fig. 2.16) curves.

The fits in this case are not as good as the ones obtained for the penicillin case (Figs. 2.10 and 2.11). This is due to the fact that the glucose oxidation mechanism is not yet completely understood and the kinetic equations are only approximate. Nevertheless, it is again possible to plot the profiles of the most important species in the gel layer and from this fit to estimate the optimum thickness of the gel layer (Fig. 2.17). For the glucose sensor, the optimum thickness appears to be 150  $\mu m$ ,

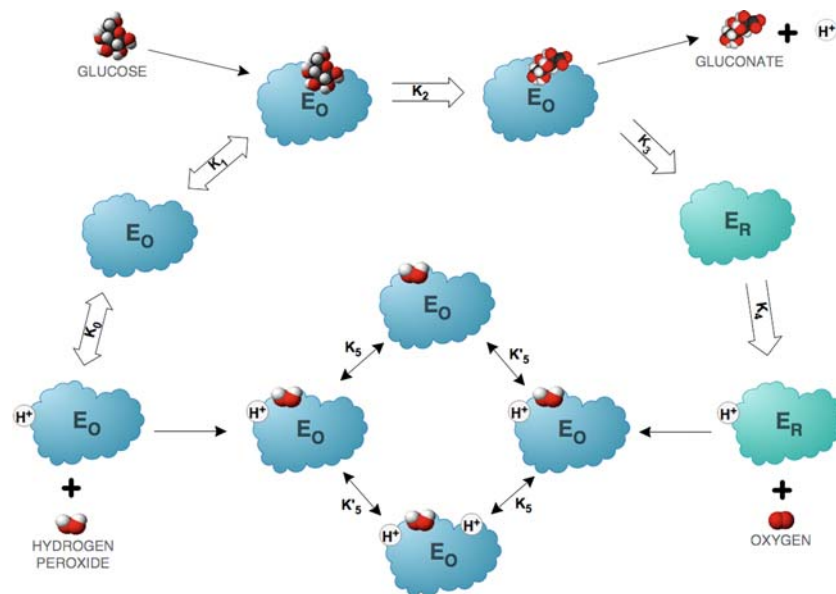


**Fig. 2.14** Glucose oxidation scheme

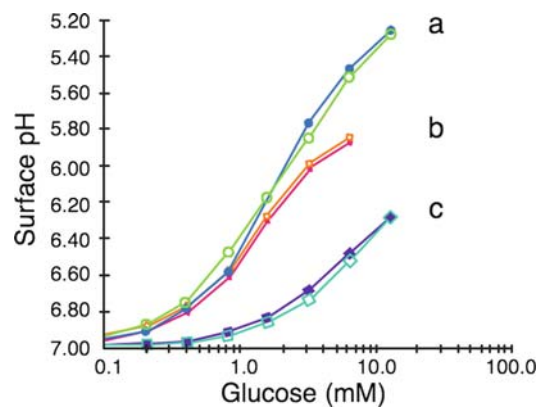


**Fig. 2.15** Theoretical (open points) and experimental (full points) calibration curve for glucose sensor for (a) 100% oxygen in 0.2 mM buffer, (b) 25% oxygen and 0.2 mM buffer, and (c) 100% oxygen and 1 mM buffer (adapted from Caras et al., 1985b, p. 1921)

under the loading conditions given earlier in this section. The most important result of this procedure is to estimate the effect of the buffer capacity and of oxygen concentration on the pH at the hydrogel/transducer boundary. This result clearly indicates that both the buffer capacity and oxygen are serious interferences and practically negate the high selectivity of the enzyme itself. This is the most serious reason why zero-flux-boundary sensors (i.e., potentiometric or optical) have failed in all but the most well-defined laboratory conditions.

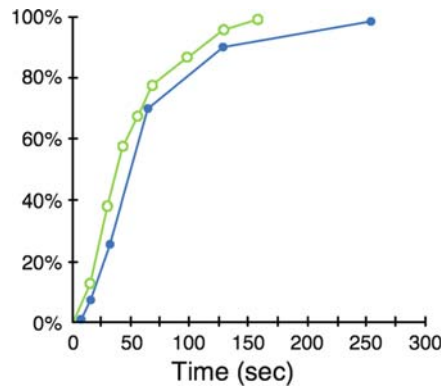


**Fig. 2.16** Theoretical (full points) and experimental (open points) time response curve for glucose sensors to step change in concentration (from 0 to 1 mM) (adapted from Caras et al., 1985b, p. 1922)

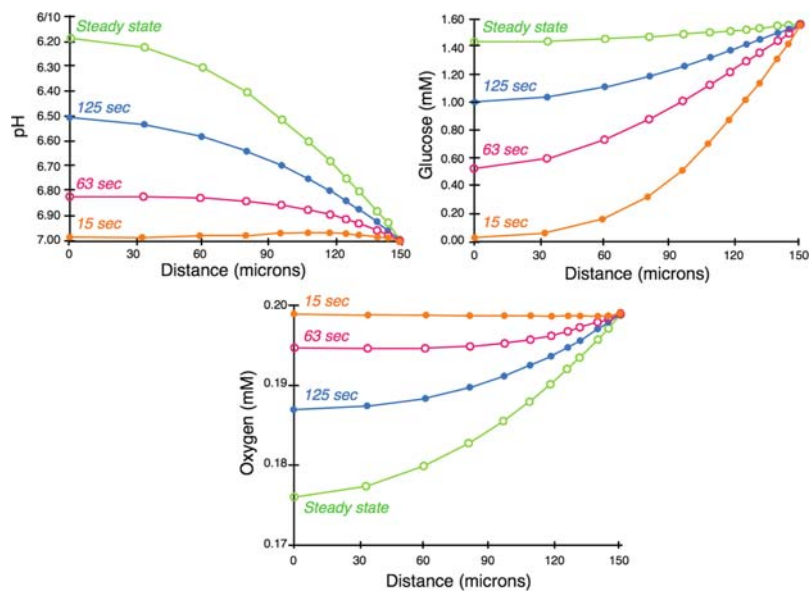


**Fig. 2.17** Evolution of concentration profiles, calculated from Figs. 2.15 and 2.16 (adapted from Caras et al., 1985b, p. 1922)

## 2.4 Mass Transport Selectivity

This form of selectivity is based on the concept of selectively blocking the access of all interfering species to the active region of the transducer. It is a form of filtration. The blockage can be achieved by size discrimination. For instance, a dialysis

membrane placed in front of a mixture containing the transducer species and other species can selectively filter out all species above a certain cutoff size. Smaller species (and presumably only the transducer species) can be allowed in.

This may work well if the process involves only electrically neutral species. However, when ions are discriminated on the basis of size, the partitioning process is affected by the Donnan potential. This potential, which we discuss more fully in Chapter 6, develops at the membrane/electrolyte interface. Another possibility is to discriminate on the basis of charge, as shown in Fig. 7.10 (see Chapter 7). Again, a porous barrier membrane is used, although here it would contain fixed, electrically charged moieties. When placed in front of the transducer, it rejects the like-charged species by electrostatic repulsion. In other words, it is a form of ion exchange membrane.

## 2.5 Design of Selective Layers

The selection, preparation, and properties of a selective layer depend largely on the type of transducer at which they will be used, as well as on the application. Those aspects are discussed in the context of the individual transduction principles. Only certain common features and procedures are included in this section.

With only a few exceptions, such as enzyme-containing layers and some ion-selective electrode membranes, the selective layers are on the order of a few micrometers thick. Therefore, common thin-film preparation techniques can be used, particularly if the uniformity of preparation is important. For layers prepared from solvents, spin-coating is the preferred technique, because it offers good control of both the thickness and uniformity. Dip-coating and drop-casting are often used for preparation of individual sensors. The rate of evaporation of the solvent influences the porosity and density of the film. It is preferable to evaporate the solvent slowly either by choosing a higher boiling point solvent, or evaporating it in an enclosed compartment against finite vapor pressure of the solvent. This is particularly important to prevent formation of the “skin,” and to achieve better adhesion to the substrate.

Vacuum deposition techniques, such as sputtering, electron beam evaporation, and plasma deposition are common. Photopolymerization and laser-assisted depositions are used for preparation of specialized layers, particularly in the fabrication of sensing arrays. Most commercial instruments have thickness monitors (Chapter 4) that allow precise control of the deposition process.

### 2.5.1 Preparation of the Substrate

Preparation of the substrate at which the layer is deposited is critically important. Some deposition techniques operate at an elevated temperature of the substrate

and/or a thermal step is included somewhere in the fabrication sequence, for example, wirebonding. The difference of the thermal expansion coefficients of the selective layer and of the substrate must always be considered. If the mismatch is too severe, delamination occurs at the substrate/layer interface and leads to device failure.

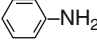
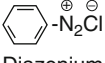
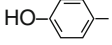
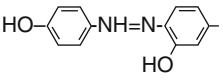
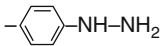
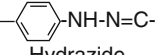
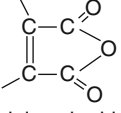
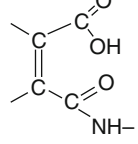
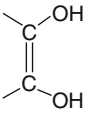
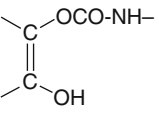
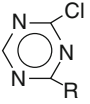
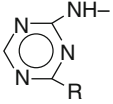
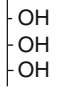
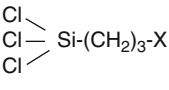
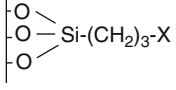
To some extent, it can be mitigated by the chemical preparation of the substrate. The first step is the removal of *dirt* (“matter in the wrong place”) which may have inadvertently contaminated the surface during one of the preceding steps. Oxygen plasma cleaning (*ashing*) generally removes organic residues. Aggressive liquid cleaners such as the “piranha solution” ( $\text{H}_2\text{O}_2/\text{H}_2\text{SO}_4$ ), can also be used, but with appropriate safety precautions. Rinsing with deionized, organics-free water is usually the final step. Use of acetone is generally not recommended because it is rarely available in sufficient purity and often leaves a thin organic residue on the substrate.

The second step is adhesion. The use of adhesion promoters is common. For oxide surfaces, silanization is by far the most popular. It can also be used for introduction of specific binding sites to the surface. It is based on the following reaction of surface hydroxyl groups with one or more reactive groups of the silane derivative, shown at the bottom of Table 2.3. Thus, a multipoint attachment, as well as introduction of the desired functional group **X** to the substrate surface, is achieved. There are many different “home kitchen” recipes that are used for the silanization. An important thing to remember is that the chloro-groups on the silane are much more reactive than the alkoxy-groups. Therefore, the reaction conditions must be adjusted accordingly. The objective of this procedure is to achieve surface activation, meaning that a monolayer of the functional groups should be the ideal result. If the silanization reaction is allowed to proceed for too long, particularly for chlorosilanes, a multilayer siloxane layer is formed that may interfere with the sensing function. Also, for the silane to react it must have an active surface hydroxyl group available. If the immediately preceding fabrication step involved temperatures above  $\sim 200^\circ\text{C}$  there may not be a sufficient number of  $-\text{OH}$  groups at the surface, resulting in poor adhesion. Therefore, a brief exposure of the oxide surface to water, followed by air-drying to remove the excess, is recommended.

Another common adhesion promotion scheme is used when thin layers of noble metals such as gold or platinum are used in the sensor. Because noble metals do not have a high affinity for oxide surfaces, their adhesion is poor and they often delaminate, particularly when exposed to solutions. Intermediate “glue metals” are used to overcome this problem. The most common mistake made is the use of chromium for this purpose. It has long been known – and just as long ignored – that chromium migrates along the grain boundaries of the deposited noble metal (Holloway, 1979). When it reaches the surface, it reacts with oxygen, covering the entire surface of the metal with  $\text{Cr}_2\text{O}_3$ . This process is surprisingly fast, and it is assisted by elevated temperature. It takes only a few hours for Cr to travel through several hundred nm of Au. The problem is less severe but also present in Pt (Josowicz et al., 1988). Chemical cleaning of the chromium-contaminated surface offers only temporary relief because the Cr migration continues. Therefore, use of Cr should be avoided. An acceptable alternative is to use a thin ( $\sim 20\text{ nm}$ ) layer of Ti. It is a more reactive



**Table 2.3** Reactive functional groups (adapted from Pace, 1981)

Reactive group I (e.g. on surface)	Intermediate	Reactive group II (e.g. on terminal reagent)	Coupling linkage "type"
$-R-NH_2$	$R'-N-C-N-R''$ (Carbodiimide)	$\begin{array}{c} O \\    \\ HO-C- \end{array}$	$-HN-C-\begin{array}{c} O \\    \end{array}$ Amide
	 Diazonium		 Diazo
		$\begin{array}{c} O \\    \\ -C- \end{array}$	 Hydrazide
$-SH$		$HS-$	$-S-S-$ Disulfide
$-SH$	$R'-N=C-N-R''$	$\begin{array}{c} O \\    \\ HO-C- \end{array}$	$-S-CO-$ Thioamide
 Maleic anhydride		$-NH_2-$	
$-COOH$	$\begin{array}{c} O \\    \\ -C-CH_2 \end{array}$	$-NH_2-$	$-CONH-$ Amide
$-CHO$	Schiff base	$-H_2N-$	$-C=N-$
	$-CNH-$	$-H_2N-$	
	Cyanuric chloride	$-H_2N-$	
			

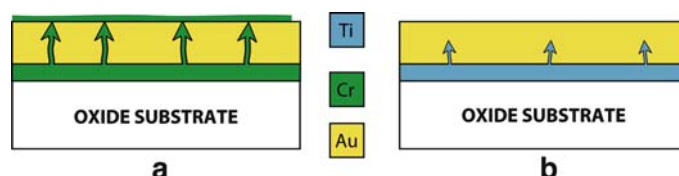


**Fig. 2.18** Adhesion promotion on noble metal substrates

metal than Cr and forms a strong bond with the oxide. The next Ti layer then alloys with the noble metal. Most important, the migration of Ti along the grain boundaries stops as soon as Ti is even partially oxidized. An interface structure that works for both Au and Pt is shown in Fig. 2.18.

Surface characterization techniques, such as photoelectron spectroscopy, can be used to verify the quality of the surface of such layers.

### 2.5.2 Immobilization of Specific Binding Sites

This section pertains particularly to proteins and other biomolecules that are used as specific binding sites in biosensors. For that purpose, these molecules have to be retained in the selective layer or at the selective surface of the sensors. Because they are usually large, one possibility is to use entrapment in a matrix. Both organic and inorganic matrices have been used for this purpose (Lev et al., 1995). However, this is not a preferred approach due to the poor control of the porosity of the matrix.

Therefore, some form of covalent attachment is preferred. In this case, it is important not to destroy the functionality of the biomolecule by affecting the immobilization at or close to its active center. This is generally achieved by using a two-step immobilization approach. In this scheme, either the surface or the matrix is first activated by introduction of some reactive functional group, and is then reacted with the linking functional group on the surface of the biomolecule. To that end, aliphatic amino groups (e.g., on lysine or arginine), thiol, or carboxylic groups have been used.

A simple, one-step immobilization technique is bulk cross-linking of the functional protein with bovine serum albumin (BSA) using glutaraldehyde as the cross-linking agent (Fig. 2.19). It is popular because of its simplicity, but it usually leads to reduction of the biological activity of the biomolecule. A cleaner and preferable approach is the two-step carbodiimide route. A partial summary of the various immobilization options was shown in Table 2.3.

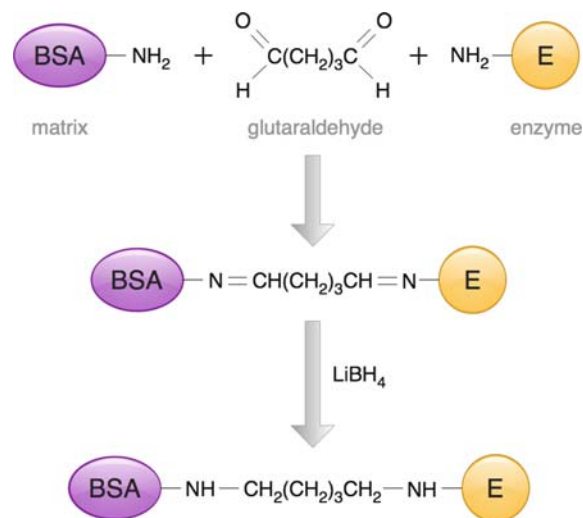


**Fig. 2.19** Glutaraldehyde cross-linking of enzyme *E* with bovine serum albumin (BSA), followed by Li borohydride stabilization

## Food for Thought #2

### *DNA Selectivity*

The formation of a duplex between fully complementary ssDNA is one of the most selective and strongest interactions between two molecules. The matching of A–T and G–C is driven by the highly specific stereochemistry of hydrogen bonding. As a result, the binding constant resulting from such multiple interactions is exceptionally high, typically greater than  $10^{10} \text{M}^{-1}$ . It has caught the attention of sensor people and tens of papers based on DNA sensing have been published, utilizing gravimetric (QCM), optical, and electrochemical transduction principles.

1. Is the selectivity of the individual A–T/G–C pair matching reflected in the overall selectivity of such sensors? Why yes or no?
2. Probe and target DNA sequences in which 10% of the bases are mismatched are effectively a “different species.” In this scenario, would the target still bind to the probe DNA?
3. Under what conditions could the high hybridization selectivity be fully utilized for direct (reversible) sensing?
4. How does the presence of 5%, 10%, and 20% mismatches affect the performance of, for example, QCM sensors?

### ***Adsorption and Absorption***

One weakness of chemical sensors based on adsorption of analyte at their surface is their poor selectivity, in other words, their vulnerability to interference from other species. Contrast this situation with the sensors having binding sites buried in the bulk of the selective layer. Such sites are accessible only by absorption.

The “surface” of a porous solid is a relative notion, dependent on the size of the species. There are porous selective layer matrices so “open” that small species can easily diffuse into their bulk without any specific interaction, yet they filter out large analytes.

5. How and where would you utilize this notion in the optimization of performance of a selective layer and what would be the trade-offs?

### ***Gas Immunosensors***

Antibodies against small molecules (haptens) can be readily prepared. It has been suggested that Ab against, for example, pesticide gas molecules can be immobilized on mass sensors and used for sensing of such gaseous compounds.

6. What will be the major interferant in such scheme?
7. Would this problem be encountered for any biosensor?
8. Assume that the hydrophobic bond is a major component of the binding interaction of the gas with the antibody binding site. What is the consequence for that type of chemical bond if performing this reaction is carried out in gas phase?

### ***Linear Solubility Energy Relationship***

Linear Energy Solubility Relationships (LSERs) are useful in the design of selective layers for mass and optical gas sensors.

9. Imagine that a polymer has been fully characterized and its free energy contribution coefficients for individual vapors A and B have been evaluated according to the LSER equation. If the polymer is fully saturated with vapor A, do you expect the coefficients for vapor B to be the same as for the polymer in the absence of vapor A? Would the evaluation of the retention times for A and B on a GC column packed with the same polymer offer any help in such a case?
10. Contrast the difference in interaction of the mixture of vapors with the solid phase used in a gas chromatographic experiment and in a direct sensing application.

## ***Molecular Imprinting***

Molecular imprinting requires multiple short-range weak interactions that act over short distances. It means that the molecular fit of the template/analyte pair must be very tight.

11. What is the effect of this requirement on removal of the template molecule from the imprint and the access of the analyte to the imprint. If it is a problem, suggest how it could be circumvented. How does Nature deal with the tight fit problem?
12. Some MIPs are created by solution polymerization. This means that the template molecule is always solvated, to some extent. Consider the role that such solvation would play in creating the imprint that is expected to mirror only the nonsolvated template molecule.
13. Are the solvation issues similar or different in the aptamer footprint forming and applications? Explain why yes or no.
14. How would you design a correct control experiment to verify that the imprinting really works?

## **Symbols**

$a\Sigma\alpha_2^H$	Term defining hydrogen bonding at an acidic site
$b\Sigma\beta_2^H$	Term defining hydrogen bonding at a basic site
$C$	Concentration
$D$	Dielectric constant
$\Delta G$	Change in free energy
$\Delta H$	Change in enthalpy
$I$	Ionization energy
$K$	Binding constant/equilibrium constant/partitioning coefficient
$K_m$	Michaelis–Menten constant
$k$	Rate constants
$L$	Thickness of a layer
$\mathfrak{R}_{pH}$	Dimensionless pH-dependent activity of enzyme
$r$	Distance
$rR_2$	Polarizability term
$\Delta S$	Change in entropy
$s\pi_2$	Polarity term
$t$	Time
$v$	Reaction velocity
$v_{max}$	Maximum reaction velocity
$x$	Distance
$z$	Charge
$\alpha$	Polarizability
$\delta$	Fraction of transferred charge

$\mu$	Dipole moment
$\Theta$	Angle
$\phi$	Thiele modulus

## References

- Abraham, M.H. (1993) *Chem. Soc. Rev.* 22, 73.
- Abraham, M.H., Andonian-Haftvan, J., Chau My Du, Diart, V., Whiting, G.S., Grate, J.W., and McGill, R.A. (1995) *J. Chem. Soc. Perkin Trans. 2*, 369.
- Absolom, D.R. and van Oss, C.J. (1986) *CCC Crit. Rev. Immunol.* 6, 1.
- Caras, S.D. and Janata, J. (1985) *Anal. Chem.* 57, 1924.
- Caras, S.D., Janata, J., Saupe, D., and Schmitt, K. (1985a) *Anal. Chem.* 57, 1917.
- Caras, S.D., Petelenz, D., and Janata, J. (1985b) *Anal. Chem.* 57, 1920.
- Diaz-Garcia, M.E. and Badia, R. (2004) Molecularly imprinted polymers for optical sensing devices. In: O.S. Wolfbeis (Ed.), *Optical Sensors*. Springer.
- Eddowes, M.J. (1985) *Sens. Actuat.* 7, 97.
- Ekedahl, L.-G., Eriksson, M., and Lundstrom, I. (1998) *Acc. Chem. Res.* 31, 249.
- Grate, J.W., Patrash, S.J., Abraham, M.H., and Chau My Du (1996) *Anal. Chem.* 68, 913.
- Haupt, K. (2004) Molecularly imprinted polymers as recognition elements in sensors. In: O.S. Wolfbeis (Ed.) *Ultrathin Electrochemical Chemo-and Biosensors*. Springer.
- Hierlemann, A., Zellers, E.T., and Ricco, A.J. (2001) *Anal. Chem.* 73, 3458.
- Holloway, P.H. (1979) *Gold Bull.* 12, 99.
- Huaiqiu Shi, Tsai W.B., Garrison, M.D., Ferrari, S., and Ratner, B.D. (1999) *Nature* 398, 593–597.
- Janata, J. and Josowicz, M. (1998) *Acc. Chem. Res.* 31, 241–248.
- Janeway, C., Travers, P., Walport, M., and Shlomchik, M. (2004) *Immunobiology: The Immune System in Health and Disease*, 6th ed. Taylor & Francis.
- Josowicz, M., Janata, J., and Levy, M. (1988) *J. Electrochem. Soc.* 135, 112.
- Lev, O., Tsionski, M., Rabinovich, L., Glezer, V., Sampath, S., Pankratov, I., and Gun, J. (1995) *Anal. Chem.* 67, 22A–30A.
- Pace, S.D. (1981) *Sens. Actuat.* 1, 475.
- Reichardt, C. (1988) *Solvents and Solvent Effects in Organic Chemistry*, 2nd ed. VCH.
- Tombelli, S., Minunni, M., and Mascini, M. (2005) *Biosens. Bioelectron.* 20, 2424–2434.
- Topart, P. and Josowicz, M. (1992) *J. Phys. Chem.* 96, 7824–7830; 8662–8666.
- Tuerk, C. and Gold, L. (1990) *Science* 249, 505–510.
- van Holde, K.E. (1985) *Physical Biochemistry*, 2nd ed. Prentice-Hall.



<http://www.springer.com/978-0-387-69930-1>

Principles of Chemical Sensors

Janata, J.

2009, XV, 373 p., Hardcover

ISBN: 978-0-387-69930-1